Structural, dielectric, and magnetic properties of $La_{0.8}Bi_{0.2}Fe_{1-x}Mn_xO_3$ $(0.0 \leq x \leq 0.4)$ multiferroics

G. Anjum,[1] Ravi Kumar,[2,a)] S. Mollah,[1,b)] D. K. Shukla,[3] Shalendra Kumar,[4] and C. G. Lee[4]

[1]*Department of Physics, Aligarh Muslim University, Aligarh 202002, India*
[2]*Centre for Material Science and Engineering, National institute of Technology, Hamirpur 177005, India*
[3]*Hamburger Synchrotronstrahlungslabor HASYLAB at Deutsches Elektronen-Synchrotron DESY, 22605 Hamburg, Germany*
[4]*School of Nano and Advanced Materials Engineering, Changwon National University, 9 Sarim dong, Changwon-641773, Republic of Korea*

(Received 3 December 2009; accepted 13 March 2010; published online 25 May 2010)

Polycrystalline multiferroic $La_{0.8}Bi_{0.2}Fe_{1-x}Mn_xO_3$ $(0.0 \leq x \leq 0.4)$ samples were synthesized by the conventional solid state reaction method. Reitveld refinement of the x-ray diffraction patterns confirms the single phase character of all the compositions with orthorhombic structure having space group *Pnma* (No. 62). Dielectric properties of the samples at temperatures 200–475 K and frequencies 500 kHz–1 MHz authenticate the stabilization of ferroelectric phase with Mn substitution. Dielectric responses of these multiferroics have been analyzed carefully, in the light of "universal dielectric response" model. While cooling from room temperature to 20 K, systematic shifts in magnetization hysteresis loops indicate the presence of exchange bias (EB) phenomenon in the system. Magnetic behavior of these samples has been briefly discussed on the basis of "EB" model for granular systems. Temperature and magnetic field dependent magnetization data demonstrate enhanced magnetization due to the Mn substitution. Magnetocapacitance measurement reveals the magnetoelectric coupling for wide range of temperature (180–280 K) and decrease in dielectric loss at high magnetic field (3 T). © *2010 American Institute of Physics*.
[doi:10.1063/1.3386527]

I. INTRODUCTION

One of the approaches to create novel materials for achieving rich functionality is to combine different physical properties in one. Ferroelectric (FE) and magnetic materials are a time honored subject of study and have led to many important technological advances till date. These seemingly distinct phenomena can coexist in certain unusual substances, termed as multiferroics. These stuffs are of vital importance, both from research as well as technology point of view. Besides their application, the fundamental physics of magnetoelectric (ME) matters is rich and fascinating. However, these types of things are very few in nature or synthesized in laboratory.[1] $BiFeO_3$ is one of the widely studied and most significant multiferroic oxide.[2–4] It is FE below $T_C \sim 1103$ K and antiferromagnetic (AFM) below $T_N \sim 653$ K, having rhombohedrally distorted perovskite structure with space group $R3c$.[5] Synthesis of $BiFeO_3$, always leads to a mixture of the main phase along with other impurity phases.[6,7] Several authors[6,8] have testified the existence of $Bi_2Fe_4O_9$ as a supplementary phase in spite of adopting the better improved techniques proposed by Sosnowska *et al.*[9] and Achenbach *et al.*[2] As a result, it is not a flawless system for device applications. Nevertheless, there are few reports on La substituted $Bi_{1-x}La_xFeO_3$ system which indicate improvement in dielectric properties as well as structural stabilization.[3,10] Furthermore, structural changes at a certain compositions of La may occur even though there are dissimilarities among the stated results.[10–13] Recently, it has also been demonstrated that the substitution of Bi^{3+} by La^{3+} in $BiFeO_3$ can effectively modify its space modulated spin structure and liberate the magnetization locked within the cycloid.[14] Another oxide $BiMnO_3$ is FE at $T_C \sim 750$ K and FM at $T_M \sim 105$ K with monoclinic (s. g. C2) structure at room temperature.[15–18] It may be synthesized with great difficulty under high pressure.[16]

Motivated from the above mentioned facts, we have tried to achieve a single phase multiferroic system by solid state reaction method without any pressure. We have introduced the compositional disorder which becomes obliging in achieving improved dielectric, magnetic, and ME properties. In order to implement this idea, we choose $LaFeO_3$ which is a rare earth transition metal (TM) oxide having orthorhombic perovskite structure with space group *Pnma*.[19] This compound is AFM in nature with Neel temperature $T_N \sim 750$ K.[19] The steadiness of the perovskite (ferrites) structure $A^{3+}FeO_3$ (where A is a rare earth element) depends on the tolerance factor t.[20–23] In $LaFeO_3$, t is less than 1. Therefore, the cubic structure transforms into the orthorhombic one and pilots to the deviation of Fe–O–Fe bond angle from 180°. This divergence in Fe–O–Fe bonds further leads to a distortion in FeO_6 octahedra. Consequently, properties can be altered/modified precisely by the choice of suitable doping element at La^{3+} and Fe^{3+} site, respectively. If we focus to the

a)On extraordinary leave from Inter University Accelerator Center, New Delhi-110067.
b)Author to whom correspondence should be addressed: Electronic mail: smollah@rediffmail.com.

 © 2010 American Institute of Physics

Downloaded 23 Aug 2011 to 131.169.95.146. Redistribution subject to AIP license or copyright; see http://jap.aip.org/about/rights_and_permissions

FE properties, it has different origin in TM based perovskite materials than the Bi-based compounds.[24] Again, the FE and FM behavior of $BiMnO_3$ is attributed by the strong covalent bonding between Bi^{3+} and O^{2-} atoms that overcomes the superexchange (SE) interactions.[25] In the present study, we have substituted Mn at Fe site in $LaFeO_3$ with Bi being in fixed proportion at La site i.e., $La_{0.8}Bi_{0.2}Fe_{1-x}Mn_xO_3$ (LBFMO) ($0.0 \leq x \leq 0.4$). 20% Bi at La site is substituted in order to introduce lone pair of electrons responsible for ferroelectricity and to get single phase samples. Possible effect on the structural and electrical properties for higher percentage of Bi (30% and 40%) at La site is in progress. The aim of present work is to inspect the modifications introduced in structural, dielectric, surface morphology, and magnetic properties by Mn substitution at Fe site in LBFMO system. We have monitored exchange bias (EB) in the system which is fascinating not only for technological application in novel magnetic memory devices, but also for a fundamental understanding of magnetic nature of compound. Prospect of coupling between FM and magnetic order parameters are also explored in the present investigations. Results suggest that both electric and magnetic domain coexist in this system and the observed Magnetocapacitance (MC) effect is due to the coupling between electric and magnetic dipoles.

II. EXPERIMENTAL DETAILS

All the samples of LBFMO ($0.0 \leq x \leq 0.4$) were synthesized using standard solid state reaction technique. The stoichiometric amounts of high purity (>99.99%) oxides of La_2O_3, Bi_2O_3, Fe_2O_3, and MnO were mixed and ground in an agate mortar till a homogeneous mixture was formed. This mixture was precalcined at 800 °C for 12 h. The precalcined powder was ground thoroughly, uniformly dye-pressed into 15 mm diameter pellets and kept in furnace at 840 °C for 12 h. These preheated pellets were again ground, palletized and sintered at 1000 °C for 24 h. Single phase nature of samples was studied by powder x-ray diffraction (XRD) pattern at room temperature using a Bruker D8 x-ray diffractometer with Cu K_α radiation. Temperature and frequency dependent dielectric properties of samples were measured with an Agilent 4285A precision LCR meter. For dielectric assessment, surfaces of pellets were polished and coated uniformly with silver paste on both sides for making electrodes. Magnetization evaluation was executed using a physical properties measurement system (Quantum design) in the temperature range of 5–320 K. Magnetization versus Magnetic field hysteresis loops were traced at different fixed temperatures ranging from 20 to 300 K. Morphological and microstructural features were investigated with FEI Quanta 200F field emission scanning electron microscope (FESEM). MC effect of the samples has been investigated at temperatures 80–280 K using a cryogen-free low temperature high magnetic field facility.

III. RESULTS AND DISCUSSION

A. XRD studies

Structure of undoped $LaFeO_3$ has been described to be orthorhombic with space group *Pnma*.[26,27] XRD data of

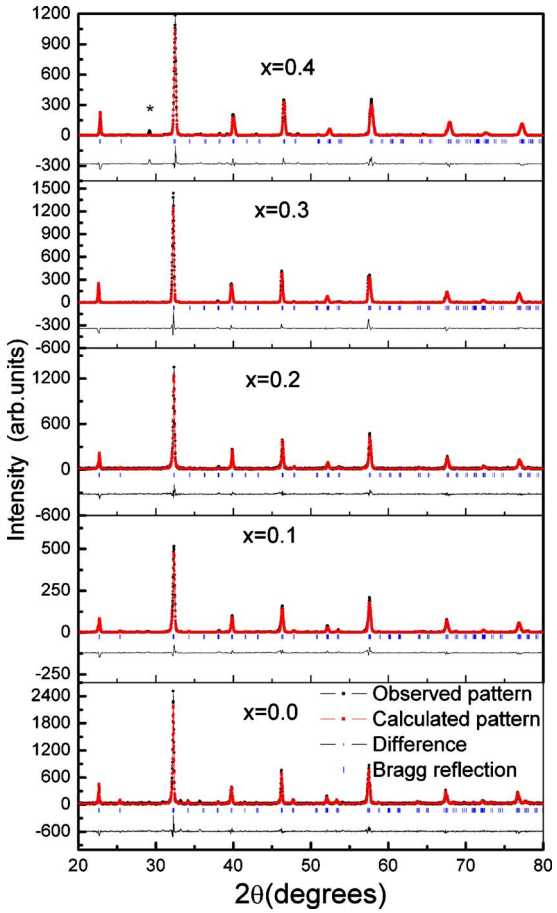

FIG. 1. (Color online) Rietveld refined XRD pattern of LBFMO ($0.0 \leq x \leq 0.4$) samples.

LBFMO ($0.0 \leq x \leq 0.4$) samples (see Fig. 1) exhibit single phase perovskite structure with no trace of impurity phases (e.g. $Bi_2Fe_4O_9$, $Bi_{25}FeO_{39}$, etc.) as revealed in the introduction. XRD pattern of samples has been refined using the Reitveld refinement method. For ease of comparison of refinement results, simulation is performed with the same initial condition as of $LaFeO_3$ with space group *Pnma*. Fitted Reitveld refined patterns for all the LBFMO ($0.0 \leq x \leq 0.4$) samples are shown in Fig. 1. Observed patterns are in good agreement with the calculated profile with χ^2 (*goodness of fit*) ~1.2. It confirms that LBFMO samples are almost in single phase and corresponds to the space group *Pnma*. Calculated lattice parameters and unit cell volume for these samples are given in Table I. It is clearly evident from the XRD analysis that there is no change in structural symmetry (orthorhombic) except the changes in lattice parameters due to Mn substitution. Shift in peaks toward higher 2θ for larger x values indicates the lattice contraction owing to the Mn substitution at Fe site leading to the distortion of Fe/MnO_6 octahedra. It is also apparent from Table I that parameter *a* is continuously lessening with the augment of Mn concentration, whereas parameters *b* and *c* illustrate minute asymmetrical variation with escalating Mn content. Overall unit cell volume is found to diminish with the proliferation of Mn concentration. This may be attributed to the smaller ionic radii of Mn^{3+} (0.58 Å) as compared to that of the Fe^{3+} (0.61 Å). One important characteristic to be noted is the appear-

Downloaded 23 Aug 2011 to 131.169.95.146. Redistribution subject to AIP license or copyright; see http://jap.aip.org/about/rights_and_permissions

TABLE I. Calculated lattice parameters and unit cell volume for $La_{0.8}Bi_{0.2}Fe_{1-x}Mn_xO_3$ $(0.0 \leq x \leq 0.4)$ samples.

Sample	Symmetry	a (Å)	b (Å)	c (Å)	Volume (Å^3)
x=0.0	Orthorhombic	5.566 80	7.848 24	5.543 91	242.211
x=0.1	Orthorhombic	5.550 01	7.832 15	5.544 48	241.010
x=0.2	Orthorhombic	5.541 20	7.832 78	5.545 98	240.712
x=0.3	Orthorhombic	5.532 07	7.832 75	5.547 68	240.388
x=0.4	Orthorhombic	5.522 45	7.832 70	5.536 52	239.486

ance of a new minor peak at $2\theta \sim 29°$ in the x=0.4 sample. It may be caused by the solubility limit of Mn in the system. This peak corresponds to the mixed phase of Mn as indexed with the joint committee on powder diffraction standards files-772 470 and 841 714. This is the reason why we limit our discussion only up to x=0.4 composition despite the improved dielectric properties with the increase in x (discussed in Sec. III B).

B. Dielectric analysis

Figure 2(a) shows the frequency (75 kHz–4 MHz) dependence of dielectric constant (ε') for the LBFMO $(0.1 \leq x \leq 0.4)$ samples at 300 K. For all samples, the ε' decreases with the increase in frequency and is consistent with combined response of orientational relaxation of dipoles and conduction of charge carriers. It may be attributable to the fact that the intra well hopping probability of charge carriers dominates and dipoles are unable to follow the field reversal in such a small interval of time at higher frequencies. It has been observed that the ε' is increasing with amplification of Mn at any particular frequency. At higher frequencies (above $\geq$500 kHz), ε' exhibits frequency independent behavior up to x=0.3. These results indicate that contributions to ε' by electrodes and grain boundaries are vanished above 500 kHz. The dielectric behavior for sample with the x=0.4 is different. Frequency independent region is not observed for this sample throughout the frequency range and value of ε' is also very large (~8263 at 75 kHz and ~2726 at 4 MHz). This may be by reason of the minor impurity phases present in this particular sample as mentioned in Sec. III A. It is additionally apparent from Fig. 2(a) that overall value of ε' for the x=0.4 material becomes almost four times to that of the undoped (x=0) one. Macroscopically, we may articulate that the substitution of Bi ion having $6s^2$ lone pair of electrons at the La site introduces ferroelectricity in the parent compound $LaFeO_3$. Dielectric property caused by polarization of the Bi $6s^2$ lone pair of electrons is in accordance with the earlier reports.[28,29] This property further gets enhanced as a result of the substitution of Fe site by Mn ion. Variation in loss tangent (tan δ) with frequency (f) at 300 K for LBFMO $(0.0 \leq x \leq 0.4)$ samples is shown in Fig. 2(b). It is evident that for a particular concentration, tan δ also decreases with the increase in f. However, the tan δ of x=0.4 sample becomes minimum first followed by a slight increase.

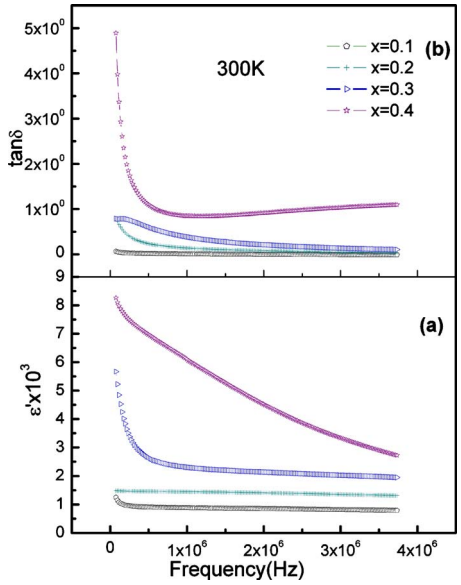

FIG. 2. (Color online) (a) Dielectric constant $(\acute{\varepsilon})$ of LBFMO $(0.0 \leq x \leq 0.4)$ samples as a function of frequency (75 kHz–4 MHz) at 300 K, and (b) Variation in tan δ vs frequency at 300 K.

In order to understand whether dielectric response of the samples is actually due to their FM nature or by some artifact effect, we have analyzed the room temperature frequency dependent (75 kHz–4 MHz) data in the light of universal dielectric response (UDR) model.[30] According to this model, localized charge carriers hopping between spatially fluctuating lattice potentials not only produce the conductivity but also may give rise to the dipolar effects. If it is true, there should be a linear behavior in the log f versus log$(f\varepsilon')$ plots. This is indeed the case at lower frequencies (f<500 kHz) for all the samples (Fig. 3). It means that UDR phenomenon is responsible for dielectric response of these samples at low frequency regime. Nonetheless, the nonlinear behavior at higher frequency region (see inset of Fig. 3) rules out the possibility of the presence of any other (electrode, Maxwell–Wagner effect, or grain boundary) contribution to the dielectric response. Catalan[31] has explained the possible origin of dielectric response in materials with nonconventional mechanisms for FE and/or magnetic ordering. It is also recognized that the systems having intrinsic capacitance will only respond at such a high frequency. The range of linear behavior also increases with the increase in Mn doping concentration. It is, therefore, concluded that the dielectric property is due to weak FE nature of these samples in high frequency region (f>500 kHz).

Figure 4 shows the ε' as a function of temperature for all samples at various fixed frequencies (500 kHz–1 MHz). It clearly demonstrates that ε' increases with Mn substitution in LBFMO samples at a fixed frequency and temperature.

Downloaded 23 Aug 2011 to 131.169.95.146. Redistribution subject to AIP license or copyright; see http://jap.aip.org/about/rights_and_permissions

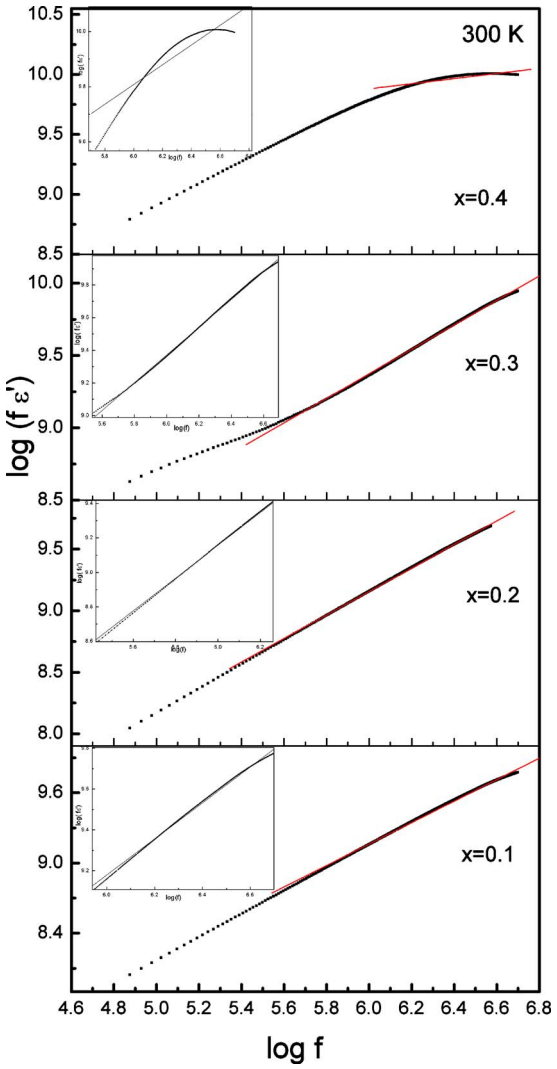

FIG. 3. (Color online) Alteration of log ($f\acute{\varepsilon}$) with log (f) for LBFMO ($0.1 \leq x \leq 0.4$) samples at 300 K in the frequency range of 75 kHz–4 MHz. Inset: enlarged view of the linear fit.

Maximum ε' (~25 453) is observed for the x=0.4 composition at a frequency of 500 kHz and temperature of 475 K. For a comparison purpose, values of ε' (at 500 kHz and 475 K) for all samples are displayed in Table II. A small dielectric anomaly is observed at ~250 K in the undoped (x =0.0) sample. However, as a virtue of Bi $6s^2$ lone pair of electrons present in system, large dielectric constant is monitored at high temperature (~475 K), which seems to have transition temperature above our measurement limit. Temperature range up to which ε' remains constant decreases with the rise of Mn doping concentration. Interestingly, we have observed that as a consequence of Mn substitution the main dielectric transition peak are found to shift toward lower temperature and ultimately a new transition (for x =0.4) seems to appear along with the primary dielectric peak. Similar behavior in $BiFe_{1-x}Mn_xO_3$ multiferroic system is also observed by Kumar and Yadav[32] and Yang *et al.*[33] In dielectric behavior of the x=0.2 and 0.3 samples, it has been found that FE transition occurs at ~423 K and 420 K, respectively. These transition peaks are well defined even at high frequency (~1 MHz) with slight shift in peak position

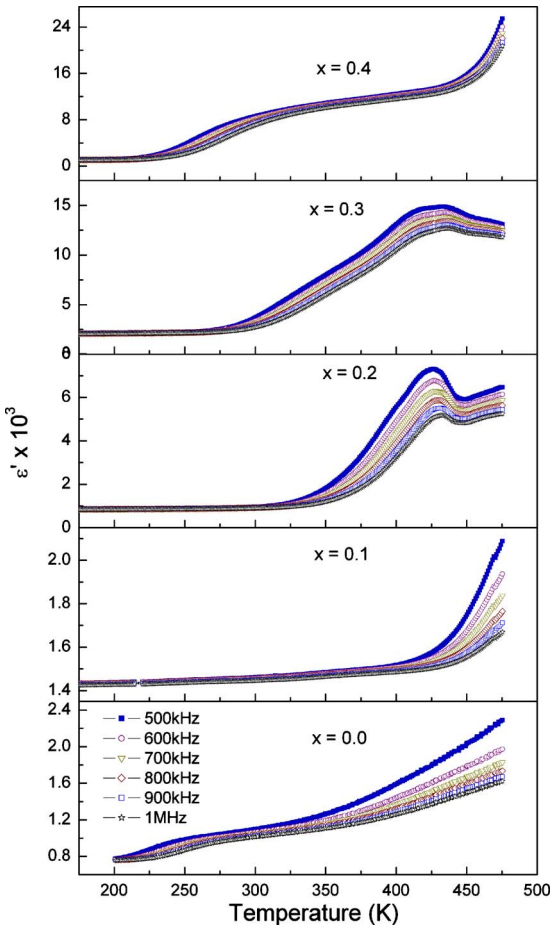

FIG. 4. (Color online) Temperature dependence of dielectric constant ($\acute{\varepsilon}$) of LBFMO ($0.0 \leq x \leq 0.4$) samples at different frequencies (500 kHz–1 MHz).

with change in f. This is an incredibly interesting feature. Usually at higher frequencies, transition peak does not remain well defined if the ferroelectricity in the system is due to electrode, Maxwell–Wagner effect or grain boundary. This further supports the actuality that dielectric behavior is basically because of weak FE nature of these samples. Temperature dependence of tan δ of the samples (Fig. 5) exhibits same behavior as those of ε' (Fig. 4), having loss peaks corresponding to the transitions in ε' versus temperature curves. Values of tan δ at 475 K and 500 kHz for all samples ($0.0 \leq x \leq 0.4$) are listed in Table II. At low temperature (<200 K), tan δ is found to be almost independent of f for all the $0.1 \leq x \leq 0.4$ samples. Slight shift in peak position with increase in f depicts presence of relaxor behavior in the system. Overall increase in values of tan δ have been ob-

TABLE II. Parameters calculated from dielectric data of $La_{0.8}Bi_{0.2}Fe_{1-x}Mn_xO_3$ ($0.0 \leq x \leq 0.4$) samples.

Sample	$\acute{\varepsilon}$ at 475 K	tan δ	ρ at 300 K (Ω-cm)
x=0.0	2300	0.59	0.27×10^9
x=0.1	2086	1.34	0.55×10^7
x=0.2	6463	0.81	0.35×10^6
x=0.3	13 066	1.25	0.39×10^5
x=0.4	25 453	3.47	0.51×10^5

Downloaded 23 Aug 2011 to 131.169.95.146. Redistribution subject to AIP license or copyright; see http://jap.aip.org/about/rights_and_permissions

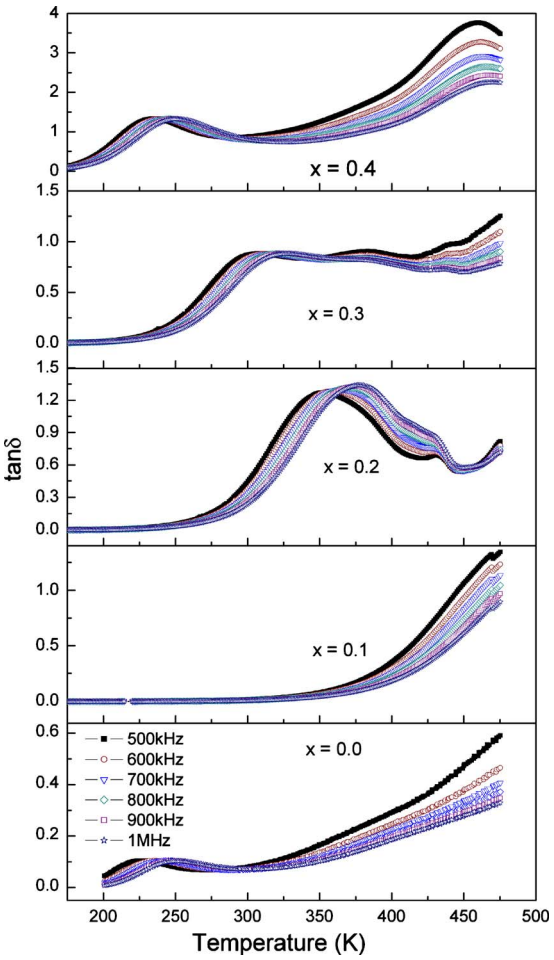

FIG. 5. (Color online) Thermal variation in tan δ for LBFMO ($0.0 \leq x \leq 0.4$) samples at different frequencies (500 kHz–1 MHz).

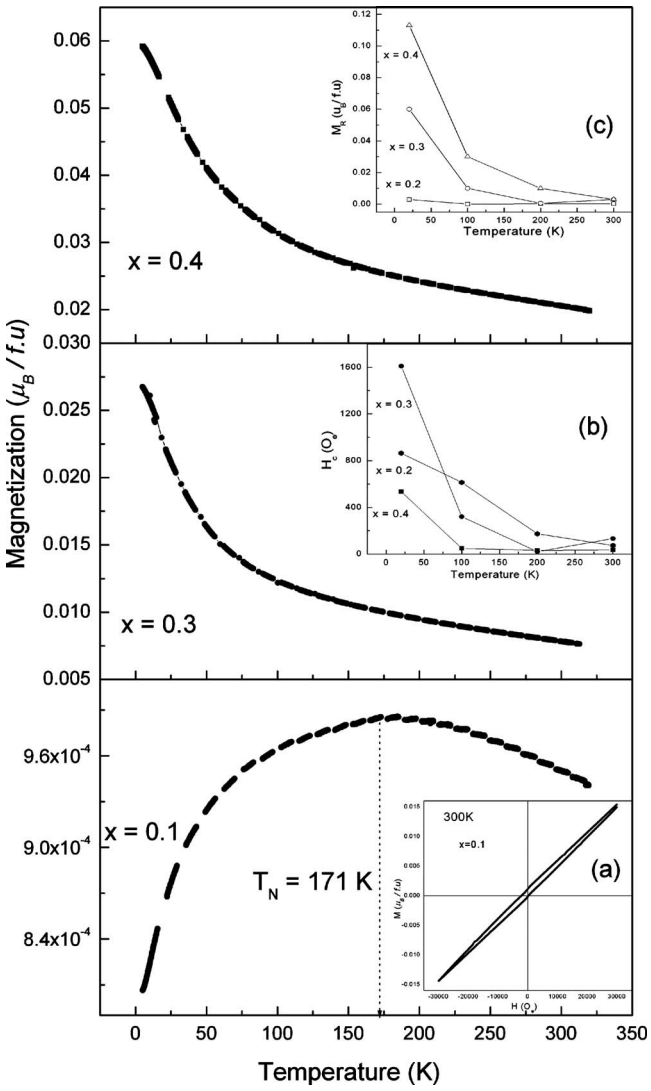

FIG. 6. FC magnetization data plotted as a function of temperature (5–320 K) for LBFMO ($0.1 \leq x \leq 0.4$) samples. Inset: (a) hysterisis behavior of sample with x=0.1. (b) Variation in coercivity with temperature. (c) Variation in remnant magnetization with temperature.

served in the Mn-substituted samples for any particular f and temperature, which may be due to an increase in dc conductivity of the materials with the Mn substitution.

C. Magnetization

Variation in magnetization with temperature (M versus T) measured in presence of an applied magnetic field of 500 Oe in the field cooled (FC) condition for samples with x =0.1, 0.3, and 0.4 is shown in Fig. 6 [insets: (a) hysteresis loop for sample with x=0.1, (b) temperature variation in coercivity, and (c) variation in remnant magnetization with temperature to be discussed later in this paragraph]. Undoped $LaFeO_3$ has been reported to be AFM in nature.[19] A notable feature is that the magnetic behavior of x=0.1 sample is completely different from others. This is attributed to the verity that Mn ions in this composition are present in +2, +3, and +4 mixed valence state (from x-ray absorption data, to be published) and this almost become +3 with very small contribution of +2 and +4 states in higher doped samples (x=0.4). It has been found that AFM transition for the x =0.1 sample occurs at $T_N \sim 173$ K. Steep increase in magnetization value is observed at low temperatures in the x =0.3 and 0.4 samples, which are demonstrating weak FM behavior. Within AFM exchange interaction, total magnetization (M_T) of the samples consist of contribution from Fe and Mn sublattices ($M_T = M_{Fe} + M_{Mn}$). Magnetic behavior of such materials which takes into account the exchange interactions among the individual magnetic moments of sublattices is best described by the Curie–Weiss law $\chi = C/(T-\theta)$, where C=Curie constant and θ=Weiss constant. It has been found that samples with x=0.3 and 0.4, obey the Curie–Weiss law and exhibit weak FM. It is clear from Fig. 6 that magnetization is growing with increase in the Mn doping in the system. This enhanced magnetization in samples may be due to two reasons. First reason is attributed to the mismatch of two magnetic ions Fe/Mn, which distorts the Fe/MnO_6 octahedra causing the frustration because of which there is difference in magnetic moments at two magnetic sublattices. Bi being a nonmagnetic ion has only a marginal effect on primary AFM exchange interactions in these samples. Another reason is that Mn substitution at Fe site may result in the mixed valence states of the Mn ions (+2, +3, and +4) to maintain charge neutrality of the system. This feature is likely associated with the verity, that presence of mixed valence states of Mn in lattice may bring in the double ex-

Downloaded 23 Aug 2011 to 131.169.95.146. Redistribution subject to AIP license or copyright; see http://jap.aip.org/about/rights_and_permissions

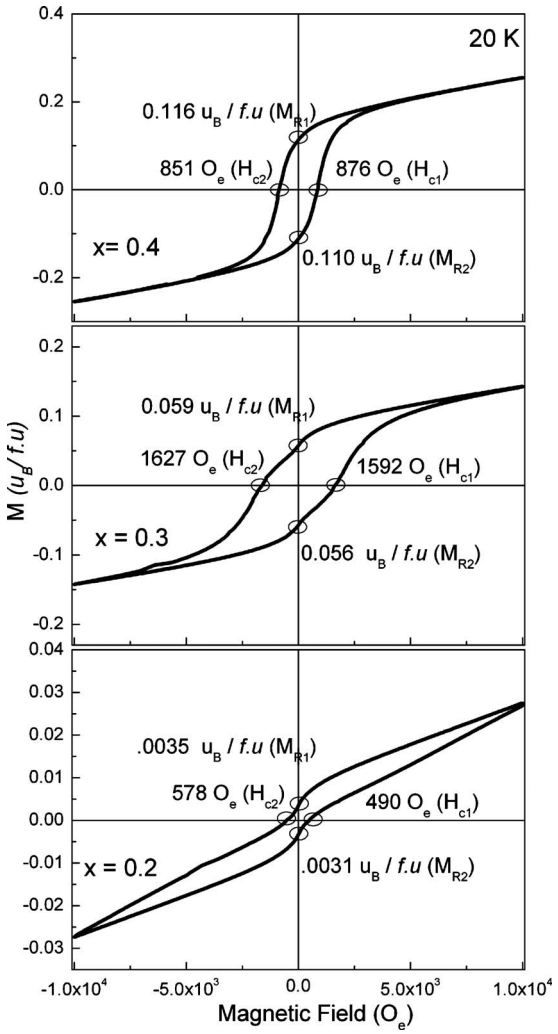

FIG. 7. M-H hysteresis curve of LBFMO ($0.1 \leq x \leq 0.4$) samples at 20 K.

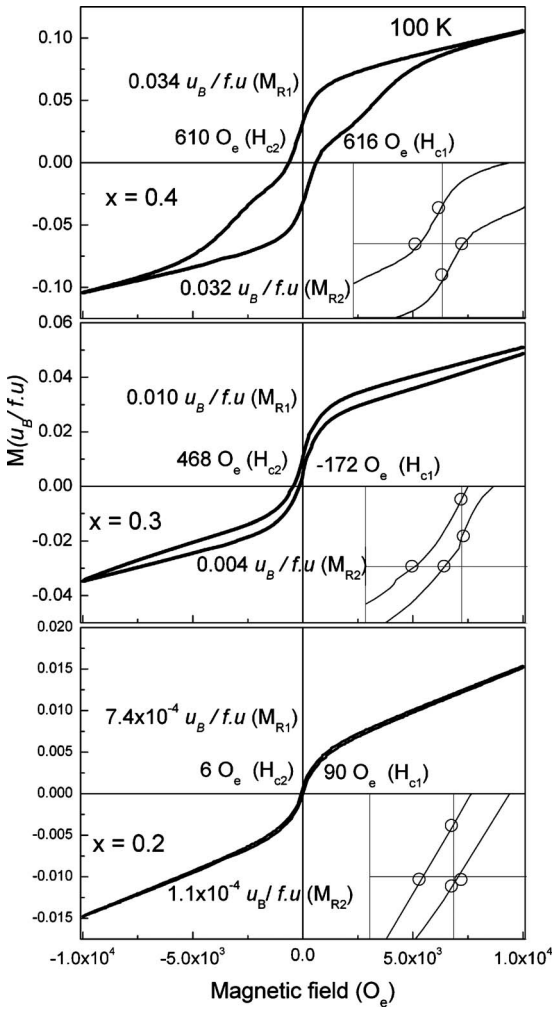

FIG. 8. Hysteresis curve of LBFMO ($0.1 \leq x \leq 0.4$) samples at 100 K. Inset: enlarged view showing the H_{EB}.

change interaction ($Mn^{2+}-O-Mn^{3+}, Mn^{3+}-O-Mn^{4+}$) and consequently weak FM. These results are in accordance with those reported by De *et al.*[34] and references therein. Also, this is in accordance with increased conductivity of samples (see Table II) due to hopping of electrons from lower to higher valence states with the increase in Mn concentration. Competition between AFM/FM lattices also affect the SE interactions ($Mn^{3+}-O-Fe^{3+}, Mn^{3+}-O-Mn^{3+}, Fe^{3+}-O-Fe^{3+}$). It might result in an incommensurate magnetic ordering in the system. This leads to an uncompensated (canted) magnetic interface that gives rise to weak FM behavior. Isothermal magnetization of LBFMO ($0.2 \leq x \leq 0.4$) samples at temperatures 20 K and 100 K are revealed in Figs. 7 and 8, respectively. Insets of Fig. 8 demonstrate the EB phenomena. Magnetization for the $x=0.0$ sample is negligibly small at all magnetic fields (not shown here) and that with $x=0.1$ exhibits the AFM behavior at 300 K [see inset of Fig. 6(a)]. Magnetic hysteresis loop have been observed in all the Mn-substituted samples (Figs. 7 and 8). It has been found that both the remnant magnetization (M_R) and coercive field (H_C) for a particular value of x increase as the samples are cooled down from higher temperatures to 20 K in the presence of field. However, the overall values of M_R increase while H_c decrease with the increase in Mn content [insets of Figs. 6(b) and 6(c)]. Most intriguing feature observed after meticulous analysis of magnetization hysteresis (M-H)_ curves of these samples is their asymmetric behavior. This indicates the presence of EB phenomenon (inset of Fig. 8), which is assumed to be associated with induced exchange anisotropy at the interface between FM and AFM phases. Magnitude of shift in curves away from $H=0$ O_e is termed as magnitude of EB (H_{EB}).[35] In general, perfect AFM systems have two sublattices that are usually identical. But EB breaks this symmetry and causes AFM sublattice to couple with FM one. Because of the FM/AFM interaction, FM spins tend to align in field direction even when the field is reduced to negative coercive field ($H=-H_c$) and eventually the field overcomes the interface interaction.[36] The present system can also be supposed to consist of two sublattices as mentioned earlier. Value of H_{EB} has been estimated from the relation $H_{EB}=(H_{c1}+H_{c2})/2$, where H_{c1} and H_{c2} (values shown in Fig. 8) are positive and negative fields, respectively, at which magnetization is equal to zero. The vertical shift is defined as $M_{EB}=(M_{R1}+M_{R2})/2$, where M_{R1} and M_{R2} are the magnetization with positive and negative points of intersection with $H=0$ O_e, respectively. Calculated values of H_{EB} and M_{EB} at different temperatures (20, 100, and 200 K) have been displayed in Table III. We further note

Downloaded 23 Aug 2011 to 131.169.95.146. Redistribution subject to AIP license or copyright; see http://jap.aip.org/about/rights_and_permissions

TABLE III. Parameters calculated from M-H curves for $La_{0.8}Bi_{0.2}Fe_{1-x}Mn_xO_3$ $(0.2 \leq x \leq 0.4)$ samples.

Samples	H_{EB} [a] (O_e)	M_{EB} [a] (μ_B/f.u.)	H_{EB} [b] (O_e)	M_{EB} [b] (μ_B/f.u.)	H_{EB} [c] (O_e)	M_{EB} [c] (μ_B/f.u.)
x=0.2	−44	0.0004	+42	3×10^{-4}	24	-1.6×10^{-4}
x=0.3	−18	0.0002	−320	31×10^{-2}	8	-1.8×10^{-4}
x=0.4	+13	0.003	+3	1×10^{-2}	−37	0.003

[a]20 K.
[b]100 K.
[c]200 K.

that the considerable EB effect is observed for samples with the x=0.2 and 0.3, and decreases in sample with the x=0.4 in the temperature range of 20–200 K. At 20 K, all samples exhibit weak FM nature (Fig. 7). It also supports the corresponding magnetization vs temperature data (Fig. 6). This feature gets decreased when the temperature is increased to 300 K. Unsaturated behavior of hysteresis curves up to magnetic fields of 1 T for x=0.2, 0.3, and 0.4 (Figs. 7 and 8), indicates that spins are highly canted.[37,38] Further evidence for the presence of two different types of contribution to magnetization (EB and sublattice effect) has been confirmed from the FESEM images as shown in Fig. 9. Overall increase in grain size along with two different types of distribution of grains has also been observed. As the Mn content is increased, number of larger grains (average grain size ~5.75 μm) increases at the expense of smaller particles (average grain size ~1.50 μm) (inset of Fig. 9). The increase in size of the FM cluster decreases the effective interface area, which weakens the exchange coupling at the FM/AFM-like interface and, thus, the EB is deteriorated with the increase in particle size and becomes small for sample with x=0.4. This explanation is consistent with the model proposed by Meiklejohn,[36] which predicts the relation to be $H_{EB} \approx J_{ex}/(M_{FM}\times t_{FM})$, where J_{ex} is the exchange constant across the FM/AFM interface per unit area, and M_{FM} and t_{FM} are the magnetization and the thickness of the FM layer, respectively. In the present observation, the average size of the FM cluster analogous to t_{FM} and M_{FM} increases with the increase in particle size, which results in a decrease in the EB field. Increase in grain size with the Mn substitution also supports to increased dielectric constant of samples (Fig. 4). From the magnetization data, we conclude that LBFMO $(0.2 \leq x \leq 0.4)$ system is having weak ferromagnetism amid the presence of EB effect.

To confirm ME coupling between magnetic and dielectric parameters, MC measurement has been performed in the temperature range of 80–300 K for a representative sample $(La_{0.8}Bi_{0.2}Fe_{0.7}Mn_{0.3}O_3)$. MC measurements for other samples (x=0.1, 0.2, and 0.4) of the series, also have been performed (not shown here) and best result is found in the sample with x=0.3. MC measurement is a standard method to confirm coupling between magnetic and FE orders.[28,31,39] Temperature dependence of observed ε' (at 123 Hz) at applied fields of 0 and 3 T is shown in Fig. 10(a). Coupling is observed for a wide range of temperature (180–280 K), rather than at a single temperature which is a good indication from application point of view. Also dielectric loss illustrates a decrease in magnitude with the application of magnetic field [Fig. 10(b)], which is the most noticeable feature observed in these materials for their application in high magnetic field. The MC has been calculated using the relation, $MC=[\varepsilon'(H,T)-\varepsilon'(0,T)]/\varepsilon'(0,T)$, where $\acute{\varepsilon}$ (H,T) represents $\acute{\varepsilon}$ at a certain magnetic field H and temperature T and $\acute{\varepsilon}$

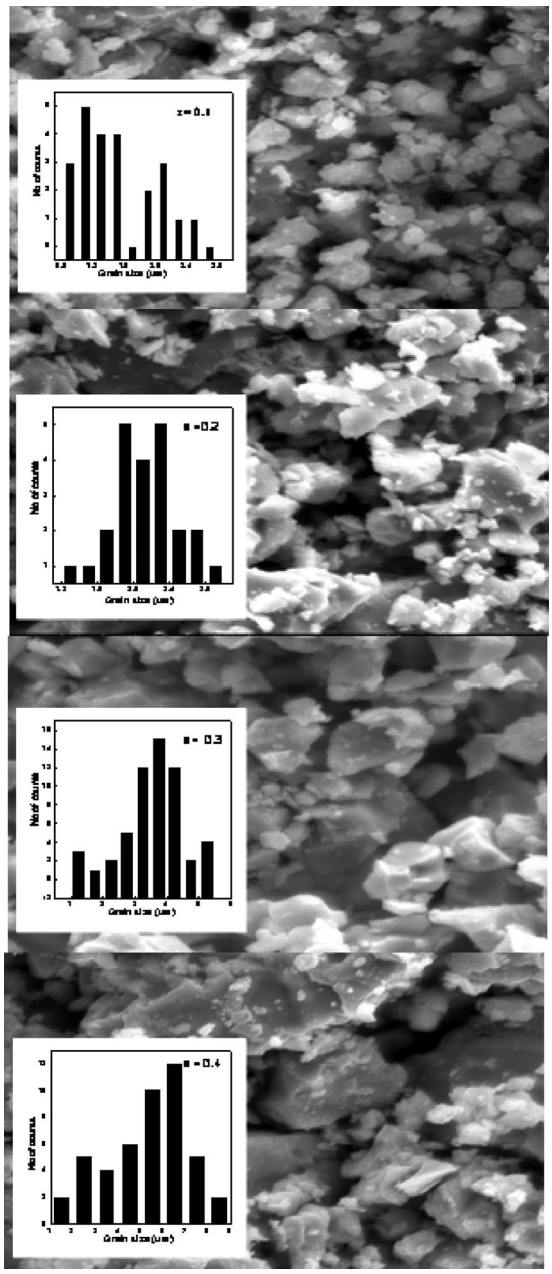

FIG. 9. FESEM micrographs of LBFMO $(0.1 \leq x \leq 0.4)$ samples taken on the scale of 10 μm. Inset: show the respective histograms of grain sizes.

Downloaded 23 Aug 2011 to 131.169.95.146. Redistribution subject to AIP license or copyright; see http://jap.aip.org/about/rights_and_permissions

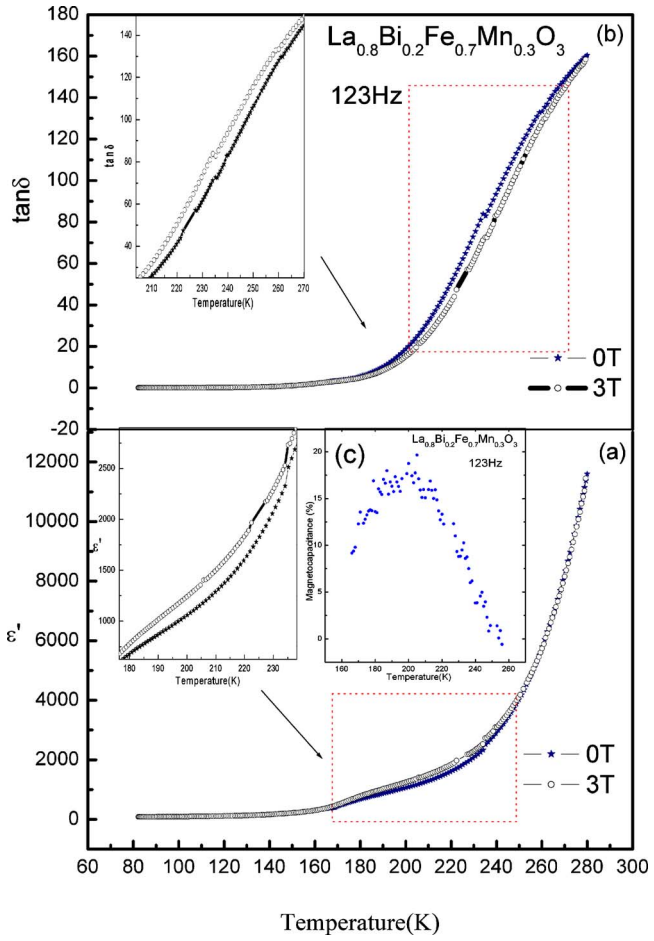

FIG. 10. (Color online) (a) Temperature variation in dielectric constant for $La_{0.8}Bi_{0.2}Fe_{0.7}Mn_{0.3}O_3$ sample in the absence and presence of a magnetic field (H=3 T). (b) Variation in tan δ in the absence and presence of magnetic field. (c) shows the percentage coupling at an applied frequency of 123 Hz. Inset: shows the enlarged part of dotted portions in [(a) and (b)].

(0, T) is $\acute{\varepsilon}$ when the external magnetic field is zero at the same temperature. Method used for the calculation of MC is parallel to that of Sun *et al.*[40] Coupling for the $La_{0.8}Bi_{0.2}Fe_{0.7}Mn0_{0.3}O_3$ composition is estimated to be about 18% at ~200 K [Fig. 10(c)], which confirms the presence of better ME coupling. Apparent MC may be due to two possible reasons. It may be due to coupling between two order parameters or because of magnetoresistance (MR) of the sample. To rule out the possibility of MR effect, we have measured it at a magnetic field of 3 T and found that it is coming out to be less than 1% (not shown here). It further verifies that the observed phenomenon is basically due to the coupling between the electric and magnetic dipoles.

IV. CONCLUSIONS

In conclusion, we have shown that the incorporation of FE host (Bi^{3+}) initiates dielectric nature in preliminary material amid phase stabilization. Substitution of Mn by magnetic ion (Fe) enhances magnetization along with ε'. Whole series of the multiferroic LBFMO (x=0.0, 0.1, 0.2, 0.3, and 0.4) samples belong to orthorhombic structure with space group *Pnma*. Unit cell volume decreases with increase in the Mn concentration due to mismatch in the ionic radii of Fe and Mn ions. Temperature dependent dielectric data exhibit higher value of ε' with the Mn substitution. Magnetic measurements confirm the favorable effect of the Mn substitution on magnetic property with enhanced magnetization. Shift in hysteresis loop proves the presence of EB in system which is important for application in magnetic devices. Noticeable feature found is the ME (18%) coupling in the system in a wide range of temperature, which is an additional aspect for making it important from application point of view.

ACKNOWLEDGMENTS

The authors are thankful to Dr. Davinder Kaur and Ashvani Kumar, Indian Institute of Technology, Roorkee, for providing the FESEM facility and Professor S. Patnaik, School of Physical Sciences, Jawaharlal Nehru University, New Delhi, for providing CLTHM facility. G. Anjum is thankful to IUAC, New Delhi, India, for providing her fellowship through the Project No. UFUP-44301.

[1] N. A. Hill, J. Phys. Chem. B **104**, 6694 (2000).
[2] G. D. Achenbach, R. Gerson, and W. J. James, J. Am. Ceram. Soc. **50**, 437 (1967).
[3] V. A. Murashav, D. N. Rakov, V. M. Ionov, L. S. Dubenko, and Y. U. Titov, Ferroelectrics **162**, 11 (1994).
[4] Y. F. Popov, A. M. Kadomtseva, G. P. Vorobev, and A. K. Zvezdin, Ferroelectrics **162**, 135 (1994).
[5] P. Ravindran, R. Vidhya, A. Kjekshus, and H. Fjellvag, Phys. Rev. B **74**, 224412 (2006).
[6] C. T. Munoz, J. P. Rivera, A. Monnier, and H. Schmid, Jpn. J. Appl. Phys. Suppl. **24**, 1051 (1985).
[7] Y. P. Wang, G. L. Yuan, X. Y. Chen, J. M. Liu, and Z. G. Liu, J. Phys. D **39**, 2019 (2006).
[8] J. K. Kim, S. S. Kim, and W. J. Kim, Mater. Lett. **59**, 4006 (2005).
[9] I. Sosnowska, T. Peterlin-Neumaier, and E. Steichele, J. Phys. C **15**, 4835 (1982).
[10] S. T. Zhang, Y. Zhang, M. H. Lu, C. L. Du, Y. F. Chen, Z. G. Liu, Y. Y. Zhu, N. B. Ming, and X. Q. Pan, Appl. Phys. Lett. **88**, 162901 (2006).
[11] Z. V. Gabbasova, M. D. Kuzmin, A. K. Zvezdin, I. S. Dubenko, V. A. Murashov, D. N. Rakov, and I. B. Krynetsky, Phys. Lett. A **158**, 491 (1991).
[12] A. V. Zalesskii, A. A. Frolov, T. A. Khimich, and A. A. Bush, Phys. Solid State **45**, 141 (2003).
[13] M. Polomska, W. Kaczmarek, and Z. Pajak, Phys. Status Solidi A **23**, 567 (1974).
[14] S.-T. Zhang, L.-H. Pang, Y. Zhang, M.-H. Lu, and Y.-F. Chen, J. Appl. Phys. **100**, 114108 (2006).
[15] G. A. Smolenskiĭ, Sov. Phys. Usp. **25**, 475 (1982).
[16] T. Kimura, S. Kawamoto, I. Yamada, M. Azuma, M. Takano, and Y. Tokura, Phys. Rev. B **67**, 180401 (2003).
[17] F. Sugawara, S. Ihda, Y. Syono, and S. Akimoto, J. Phys. Soc. Jpn. **25**, 1553 (1968).
[18] M. D. Santos, S. Parashar, A. R. Raju, Y. S. Zhao, A. K. Cheetham, and C. N. R. Rao, Solid State Commun. **122**, 49 (2002).
[19] C. N. R. Rao, O. Prakash, and P. Ganguly, J. Solid State Chem. **15**, 186 (1975).
[20] A. S. Bhalla, R. Guo, and R. Roy, Mater. Res. Innovations **4**, 3 (2000).
[21] J. R. Sun, G. H. Rao, and J. K. Liang, Appl. Phys. Lett. **70**, 1900 (1997).
[22] H. Y. Hwang, S. W. Choeng, R. G. Radaelli, M. Marezio, and B. Batlog, Phys. Rev. Lett. **75**, 914 (1995).
[23] J. M. De Teresa, M. R. Ibarra, J. Garcia, J. Blasco, C. Ritter, P. A. Algarabel, C. Marguina, and A. del Moral, Phys. Rev. Lett. **76**, 3392 (1996).
[24] D. I. Khomskii, J. Magn. Magn. Mater. **306**, 1 (2006).
[25] W. Prellier, M. P. Singh, and P. Murugavel, J. Phys.: Condens. Matter **17**, R803 (2005).
[26] D. V. Efremov, J. Van den Brink, and D. I. Khomskii, Nature Mater. **3**, 853 (2004).
[27] R. Kumar, R. J. Choudhary, M. W. Khan, J. P. Srivastava, C. W. Bao, H. M. Tsai, J. W. Chiou, K. Asokan, and W. F. Pong, J. Appl. Phys. **97**, 093526 (2005).

Downloaded 23 Aug 2011 to 131.169.95.146. Redistribution subject to AIP license or copyright; see http://jap.aip.org/about/rights_and_permissions

[28]N. E. Rajeevan, P. P. Pradyumnan, R. Kumar, D. K. Shukla, S. Kumar, A. K. Singh, S. Patnaik, S. K. Arora, and I. V. Shvets, Appl. Phys. Lett. **92**, 102910 (2008).
[29]D. K. Shukla, S. Mollah, R. Kumar, P. Thakur, K. H. Chae, W. K. Choi, and A. Banerjee, J. Appl. Phys. **104**, 033707 (2008).
[30]A. K. Jonscher, J. Phys. D **32**, R57 (1999).
[31]G. Catalan, Appl. Phys. Lett. **88**, 102902 (2006).
[32]M. Kumar and K. L. Yadav, Appl. Phys. Lett. **91**, 242901 (2007).
[33]C. H. Yang, T. Y. Koo, and Y. H. Jeong, Solid State Commun. **134**, 299 (2005).
[34]K. De, M. Patra, S. Majumdar, and S. Giri, J. Phys. D **40**, 7614 (2007).
[35]D. Fiorani and L. Del Bianco, A. M. Testa, and K. N. Trohidou, J. Phys.: Condens. Matter **19**, 225007 (2007).
[36]W. H. Meiklejohn and C. P. Bean, Phys. Rev. **102**, 1413 (1956); W. H. Meiklejohn, J. Appl. Phys. **33**, 1328 (1962).
[37]A. K. Kundu, P. Nordblad, and C. N. R. Rao, J. Phys.: Condens. Matter **18**, 4809 (2006).
[38]V. R. Palkar, D. C. Kundaliya, and S. K. Malik, J. Appl. Phys. **93**, 4337 (2003).
[39]A. K. Singh, S. D. Kaushik, B. Kumar, P. K. Mishra, A. Venimadhav, V. Siruguri, and S. Patnaik, Appl. Phys. Lett. **92**, 132910 (2008).
[40]Z. H. Sun, B. L. Cheng, S. Dai, L. Z. Cao, Y. L. Zhou, K. J. Jin, Z. H. Chen, and G. Z. Yang, J. Phys. D **39**, 2481 (2006).

Downloaded 23 Aug 2011 to 131.169.95.146. Redistribution subject to AIP license or copyright; see http://jap.aip.org/about/rights_and_permissions